Strong induced-fit binding of viologen and pyridine derivatives in adjustable porphyrin cavities

Alexander B. C. Deutman, Cyrille Monnerau, Jan M. M. Smits, René de Gelder, Johannes A. A. W. Elemans,* Roeland J. M. Nolte,* and Alan E. Rowan*

Radboud University Nijmegen, Institute for Molecules and Materials, Heyendaalseweg 135, 6525 AJ Nijmegen, The Netherlands. E-mail: J.Elemans@science.ru.nl, R.Nolte@science.ru.nl, A.Rowan@science.ru.nl

Abstract:

The synthesis and binding properties of new porphyrin cage compounds consisting of a rigid diphenylglycoluril part, which is connected via flexible bis(ethyleneoxy) spacers to a (metal-) porphyrin 'roof', are reported. Binding of viologen guests and pyridine ligands in these porphyrin cages are accompanied by significant conformational reorganizations of the hosts. Despite these structural changes, association constants are still very high, revealing that not only receptors that bind guests according to a lock-and-key mechanism but also those that bind guests via an induced-fit mechanism can exhibit strong binding.

Keywords: host-guest chemistry • supramolecular chemistry • rotaxanes • induced-fit binding • viologens

Introduction

In search for new synthetic catalysts that function according to the principles of enzymes, different types of catalytically active receptor molecules have been developed,[1] many of which consist of metal porphyrins that are covalently connected to a substrate-recognizing cavity.[2-12] We have previously reported on the synthesis and guest binding properties of so-called 'porphyrin clips', cavity molecules based on diphenylglycoluril that are capped with a porphyrin roof (**$H_2$2**, **$H_2$3**).[13] Insertion of a manganese center in the porphyrin plane of **$H_2$2** to give **Mn2** turned the host molecule into a catalyst for the epoxidation of alkenes. When the outside of the host was shielded by coordinating a bulky axial ligand to the manganese center, the catalysis was forced to take place on the inside of the cavity.[14,15] Using this approach, a mimic of so-called processive enzymes such as DNA polymerase and λ-exonuclease, was developed. These enzymes duplicate or modify a DNA strand while remaining attached

to their polymeric substrate..[16] It was shown that catalyst **Mn2** was capable of oxidizing the double bonds of the synthetic polymer polybutadiene by a mechanism in which the catalyst moves along the polymer chain. [17] Unlike many of the natural processive catalysts that operate in a sequential fashion, the oxidation of polybutadiene by **Mn2** seemed to be a random process, since the rate of movement over the polymer chain was several orders of magnitude larger than the turnover rate of the catalytic reaction.[18]

With the objective to further control the threading of the catalyst on the polymer, i.e. by achieving a more induced fit-like binding of the host during the process of gliding along the polymer chain, a new porphyrin clip molecule **1** was designed, which has a larger and more flexible cavity than host **2**. By studying **1** and its catalytically active Mn(III) derivative it is expected that new insights in the mechanisms of the threading and catalysis will be obtained. In this paper, the synthesis, conformational analysis, and binding properties of this new flexible porphyrin clip molecule is described. The results of the threading and catalysis experiments will be reported elsewhere.

Results and Discussion

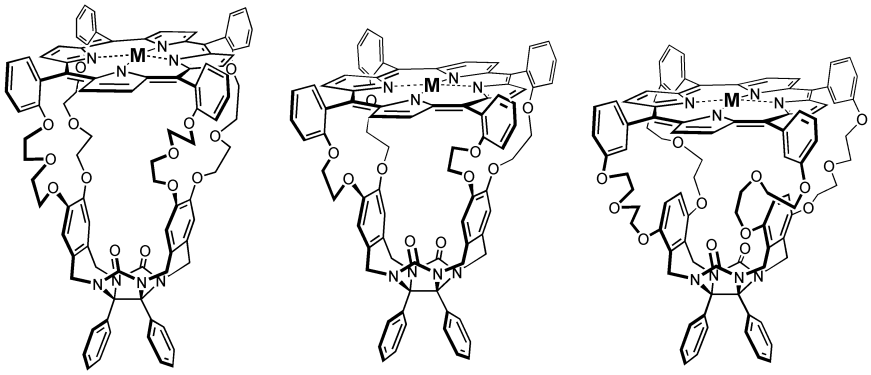

$H_2$1 **M** = H_2
Zn1 **M** = Zn
Mn1 **M** = Mn

$H_2$2 **M** = H_2
Zn2 **M** = Zn
Mn2 **M** = Mn

$H_2$3 **M** = H_2
Zn3 **M** = Zn

Design. A catalyst ideally consists of a substrate-recognizing binding region, located in the proximity of a catalytically active site. Interactions between the substrate(s) and the binding region during the process of catalysis might result in regio- or stereoselectivity of the catalytic reaction. This concept has been shown to work in many examples of catalysis involving supramolecular catalysts[19-23] and templating capsules.[24-27] In our group it was demonstrated that the *cis*/*trans* ratio of the formed epoxides in the oxidation of olefins by **Mn2** can be influenced by directing the catalysis to the inside or the outside of its cavity.[14,17] In natural enzymatic systems, the mechanisms of substrate recognition, catalysis, and product release are explained in terms of 'lock-and-key',[28,29] induced-fit,[30] conformational selection,[31,32] or a combination of these three. Crucial steps in enzymatic catalysis are a high selectivity for the substrate, the

ability to lower the activation energy of the transition state of the reaction compared to an uncatalyzed reaction, and finally little affinity of the enzyme for the product, thereby promoting product release. Whereas the induced-fit theory is most frequently used to explain the working mechanisms of many natural enzymatic systems, so far most synthetic supramolecular catalysts function according to a 'lock-and-key' mechanism, in which the preorganization of a rigid molecular host determines the binding of substrate molecules and little conformational changes are possible during the process of catalysis. In this respect **Mn2** also is a very rigid cage molecule, and therefore operates in a lock-and-key fashion. Sanders has suggested[33] that the rigidity of most synthetic supramolecular catalysts is a drawback for catalysis and that more flexible systems might well improve the catalytic performance, because they allow a conformational response to the catalytic process, comparable to enzymes in Nature. In our group the more flexible porphyrin host **3**,[13] which compared to **H$_2$2** has larger and more flexible spacers connected to the *meta*-positions of the porphyrin phenyl groups and to the o-xylylene positions of the cavity side-walls, had already been synthesized. It showed a high degree of induced-fit behaviour for the binding of guest molecules,[13] but the association constants for a large number of guests were significantly lower than those observed for the binding of guests in rigid host **2**, because the cavity of **3** is too wide to provide ideal stabilizing interactions to the guest molecules. In order to obtain a catalyst that binds guests strongly to the inside of its cavity while still operating according to an induced fit-mechanism, porphyrin host **1** was designed. When compared to host **2**, it has extended oxyethylene spacers in a crown ether-like arrangement connected to the *ortho*-phenyl positions of the porphyrin. The compound is expected to have a larger, but narrower cavity than host **3**, which will be better suited for the complexation of guest molecules, whereas the extra oxyethylene unit in the spacers will provide the molecule with the flexibility needed for induced-fit binding.

Synthesis. The synthesis of **H$_2$1** (Scheme 1) started from catechol (**4**) which was alkylated with 2-(2-chloroethoxy)-ethanol (**5**) in the presence of K_2CO_3 in DMF to form diol **6**[34] in nearly quantitative yield. Diol **6** was treated with *p*-toluenesulfonyl chloride in pyridine to give the ditosylate **7** in a yield of 62%.[35] A Friedel Crafts alkylation between tetrakis(chloromethyl) diphenylglycoluril **8**[36] and ditosylate **7** in 1,2-dichloroethane, using tin tetrachloride as a Lewis acid catalyst, gave tetratosylated clip **9** in a moderate 23% yield. In addition to **9**, a mono-walled compound was obtained and a mixture of isomers of **9** in which the aromatic side-walls were not connected via the 4,5- but via the 3,4-positions. The different products could be separated and purified by column chromatography followed by precipitation in *n*-hexane. Tetratosylated clip **9** was reacted with 5,10,15,20-tetrakis(*meso*-*o*-hydroxyphenyl)porphyrin **10** in DMF under basic conditions to give the free base porphyrin clip **H$_2$1** in 10-15% yield, after purification by column chromatography, preparative TLC, and precipitation in *n*-

hexane. **H₂1** was nearly quantitatively converted to the corresponding zinc derivative **Zn1** by a reaction with an excess of zinc acetate dihydrate in a 1:1 mixture of dichloromethane and methanol.

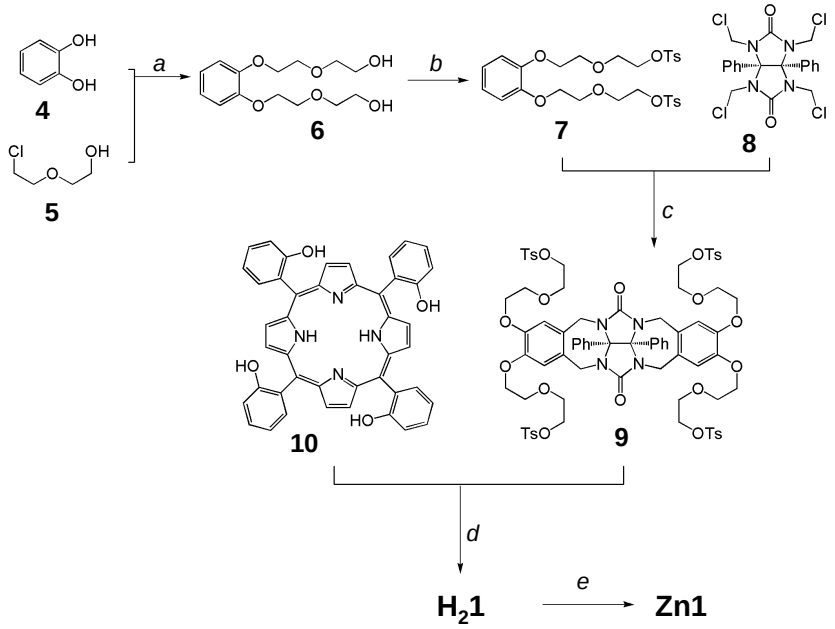

Scheme 1 Synthesis of **H₂1** and **Zn1**. Reagents and conditions: a) K_2CO_3 , DMF, 100ºC, 12h, 98%; b) TosCl, pyridine, 2h, 62%; c) $SnCl_4$, 1,2-dichloroethane, reflux, 16 h, 23%; d) K_2CO_3, DMF, 110ºC 10-15%; e) $Zn(OAc)_2.2H_2O$, MeOH/DCM 1:1 (v/v) 96%.

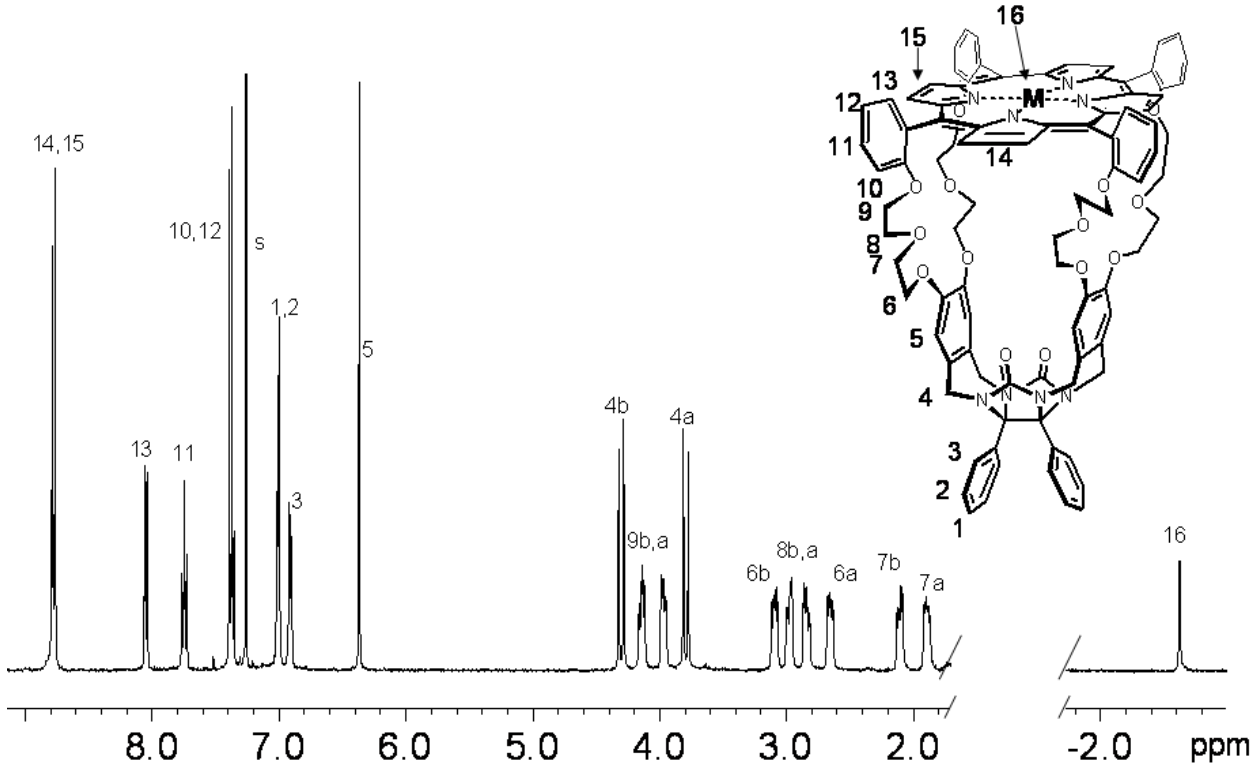

Figure 1 Proton assignments in the 400 MHz ^{1}H-NMR spectrum of **H₂1** (M = 2H) in $CDCl_3$.

Structural analysis. The structure of **H$_2$1** was elucidated with ^{1}H NMR spectroscopy. All proton resonances could be assigned with the help of COSY and 2D-ROESY techniques. The ^{1}H NMR spectrum of **H$_2$1** in $CDCl_3$ at room temperature (Figure 1) reveals that the compound has C_{2v} symmetry. For all eight oxyethylene protons in the spacer region separate signals can be observed. Compared to the oxyethylene proton signals of ditosylate **7**, the proton signals of H-6, H-7 and H-8 exhibit a large upfield shift of –1 to –2 ppm, which can be ascribed to the shielding effect of the porphyrin ring current, suggesting that these protons are all in the direct proximity of the porphyrin surface. Molecular modeling calculations of **H$_2$1** based on the nOe constraints observed in the 2D-ROESY spectrum predict an average non-symmetric conformation for the molecule, in which the clip framework is arranged in a twisted fashion underneath the porphyrin roof, with the crown ether spacers filling up the space between these two moieties (Figure 2). This non-symmetry is not observed in the ^{1}H NMR spectrum at room temperature, because the exchange of the different conformations is fast on the NMR timescale. Variable temperature NMR experiments in $CDCl_3$ demonstrated that it is possible to freeze out non-symmetrical conformations of the molecule. In the 500 MHz ^{1}H NMR spectrum of **H$_2$1** in $CDCl_3$ at 218 K, a doubling of the shifts was observed for protons throughout the molecule (Figure 3b). The downfield shifted resonances of the spacer protons (most significantly those of H-7a and H-7b, which are closest to the porphyrin) suggest that at a lower temperature they are further away from the porphyrin plane, which indicates that the molecule adopts a more opened conformation upon cooling.

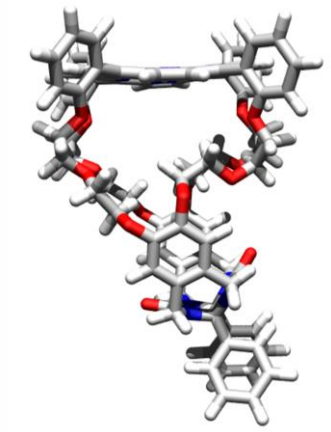

Figure 2 Computer-modeled structure of **H$_2$1** in $CDCl_3$ at room temperature, based on the ^{1}H-NMR, COSY and 2D-ROESY spectra.

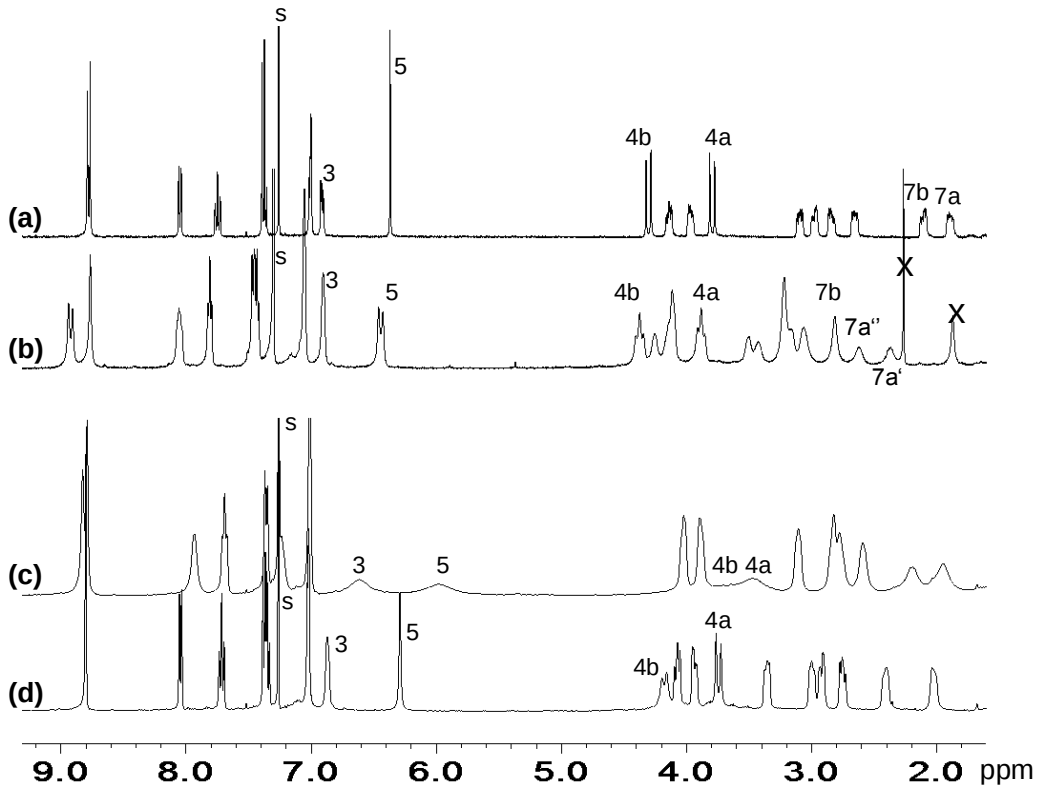

Figure 3 400 MHz (a, c and d) and 500 MHz (b) ^{1}H-NMR spectra of **$H_2$1** at (a) 298 K and (b) 218 K in $CDCl_3$, and of **Zn1** (*c*) in the presence of 0.7 equivalents of water in $CDCl_3$ and (*d*) in $CDCl_3$ saturated with water. See Figure 1 for proton numbering.

The insertion of a zinc ion in the porphyrin to give **Zn1** caused a broadening of signals over the entire range of the ^{1}H NMR spectrum in $CDCl_3$, most dramatically for the signals of the side-wall protons H-5, the phenyl proton H-3, and the benzylic protons H-4a and H-4b (Figure 3). These signals are shifted upfield compared to the signals of **$H_2$1**, indicating that in **Zn1** the clip moiety is located closer to the porphyrin roof. This effect is proposed to be the result of intramolecular coordination of one of the crown ether oxygen atoms of the spacer to the zinc ion in the porphyrin. A 2D-ROESY NMR measurement showed NOE contacts between many of the crown ether protons and the porphyrin β-pyrrole protons (H-14, H-15), which confirms the proposed closed conformation of the molecule. Further evidence for the intramolecular coordination interaction was obtained from the UV-vis spectrum of **Zn1** in $CHCl_3$ (Figure 4), in which the porphyrin Soret and Q bands showed red-shifts of 7 and 13 nm, respectively, compared to these bands in the UV-vis spectrum of **Zn2**, in which such an interaction is absent. These observed red-shifts are typically observed when oxygen atoms (such as [1,4]dioxane, tetrahydrofuran and diethylether) are coordinated to the zinc center in porphyrins.[37] The non-symmetric shape of the Soret band of **Zn1** indicates that the molecules are present as a mixture of conformers in which either the intramolecular coordination is absent (absorption maximum at 419 nm) or in which it is present and the molecule adopts a closed conformation (absorption maximum at 429 nm), roughly in a 1:2 ratio as could be determined by

deconvolution (Figure 4). In order to rule out that the observed spectral properties are simply a result of coordination of water to the zinc ion on the inside of the cavity (an effect which has been observed in X-ray structures of some crown ether-functionalized porphyrins[38]), a ^{1}H NMR titration of **Zn1** with water was performed in $CDCl_3$. Although the titration revealed a weak coordination of this ligand (K_a = 30 M^{-1}) to the inside of the cavity, it induced an opening of the cavity rather than a closing, as can be concluded from the downfield shift of the resonances of H-3, H-4 and H-5 (Figures 3c, d). These observations indicate that water coordination does not account for the observed closed conformation of **Zn1**.

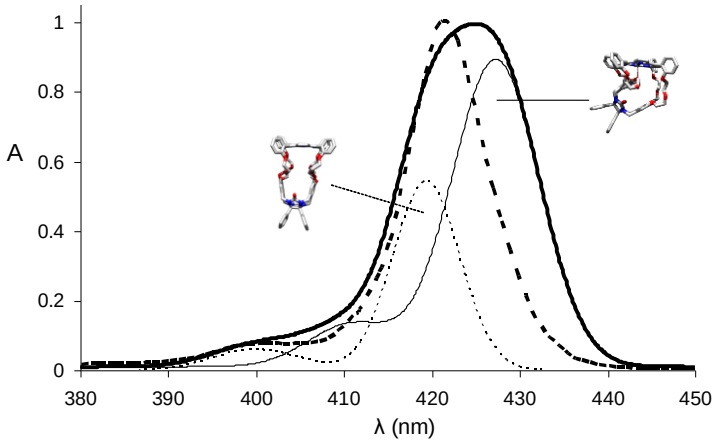

Figure 4 Selection of normalized UV-vis spectra in chloroform of **Zn1** (▬), **Zn2** (- - -), and the contributions, calculated by deconvolution, of the intramolecular zinc-oxygen coordinated (——) versus the non-coordinated (- - -) conformers of **Zn1** to the total spectrum.

Binding properties. Cavity-containing porphyrin receptor molecules based on diphenylglycoluril are known to be capable of binding small aromatic guest molecules by a variety of interactions, viz., by hydrogen bonding, π–π interactions,[39] van der Waals interactions, dipole interactions, and in the case of a Zn(II) ion present in the porphyrin, by complexation of ligands to the metal center. In the following sections the complexation behaviour of pyridine and viologen substrate molecules to hosts **H$_2$1** and **Zn1** will be investigated.

Binding of pyridine derivatives. A number of ^{1}H NMR and UV-vis titrations were carried out in $CDCl_3$/CD_3CN 1:1 (v/v) and $CHCl_3$/CH_3CN 1:1 (v/v), respectively, to investigate the binding of pyridine-containing substrates **P1**-**P5** to host **Zn1**. Upon coordination of all the pyridine ligands, the UV-vis spectra showed very similar 3-4 nm red-shifts of the porphyrin Soret band. In addition, the presence of several isosbestic points indicated the formation of well-defined host-guest complexes.

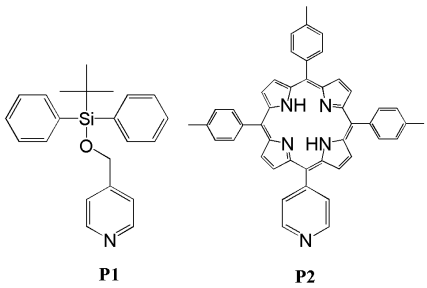

P1 **P2**

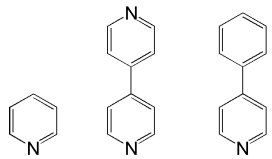

P3 **P4** **P5**

Table 1 Association constants K_a and binding free energies ΔG^o of complexes between **Zn1** and pyridine ligands **P1**-**P5**

Guest	K_a (M^{-1})	ΔG^o (kJ $mole^{-1}$)
P1[a,b]	$(5.5 \pm 0.3) \times 10^2$	–15.6
P2[a]	$(3.5 \pm 0.7) \times 10^2$	–14.5
P3[a,b]	$(3.2 \pm 0.8) \times 10^3$	–20.0
P4[b,c]	$(3.1 \pm 1.0) \times 10^4$	–25.6
P5[b]	$(2.8 \pm 0.5) \times 10^4$	–25.4

[a]Determined by a ^{1}H-NMR titration in $CDCl_3/CD_3CN$ 1:1 (v/v) or [b]by a UV-vis titration in $CHCl_3/CH_3CN$ 1:1 (v/v). [c]The bivalent character of **P4** was taken into account by dividing the experimentally obtained value of the association constant by a factor 2.

Upon the addition of each of the ligands, the broad signals in the ^{1}H NMR spectrum of **Zn1** sharpened, indicating a replacement of the intramolecular zinc-oxygen coordination by the intermolecular coordination of the pyridine ligands. Bulky pyridines **P1** and **P2** are too large to fit inside the cavity and as a result they can only coordinate to the zinc ion on the outside. Coordination of these ligands to **Zn1** induced in both cases identical shifts in the ^{1}H NMR spectra, which indicates that similar binding geometries occur. The downfield shifts of the signals of protons H-3, H-4 and H-5 indicate that the cavity adopts a more opened conformation, very similar to that observed for $\mathbf{H_2 1}$, which is confirmed by the nearly identical resonances observed for **Zn1** in the ^{1}H NMR spectra (Table 2). The calculated association

constants for **P1** and **P2** with **Zn1** are relatively low (K_a for **P1** = 550 M^{-1}, K_a for **P2** = 350 M^{-1}), which is due to the absence of additional stabilizing interactions by the cavity and to the competition of the intramolecular zinc-oxygen coordination with the coordination of the ligands. Pyridine (**P3**) coordinates predominantly on the inside of the cavity. In the ^{1}H-NMR spectra of the complex, the signals of the oxyethylene protons H-6 and H-7 have shifted downfield, which indicates that their position in close proximity to the porphyrin has been occupied by the ligand (Table 2). The association constant (K_a = 3200 M^{-1}) is of the same order of magnitude as those of other pyridine-to-zinc-porphyrin association constants in this solvent mixture,[40] which suggests that **P3** only experiences little extra stabilizing interactions despite its position inside the cavity of **Zn1**. As opposed to the complexes of **P3** with **Zn2** and **Zn3**, which are extra stabilized by favourable π–π interactions, leading to high association constants (typically K_a **Zn2-P3** ($CHCl_3$) = 1.1 × 10^5 M^{-1} , K_a **Zn2-P3** ($CHCl_3$/CH_3CN 1:1 (v/v)) = 7.5 × 10^4 M^{-1}, and K_a **Zn3-P3** ($CHCl_3$) = 1.4 × 10^4 M^{-1}),[13] the complex between **Zn1** and **P3** apparently does not experience these extra stabilizing interactions, probably because the complex cannot adopt a geometry in which the pyridine ring is located in between the cavity side-walls due to the longer crown ether spacers. Molecular modeling indicated that 4,4'-bipyridine (**P4**) and 4-phenylpyridine (**P5**) would be large enough to be accommodated with an ideal fit inside the cavity of **Zn1**. Upon the addition of **P4** or **P5** to **Zn1**, the ^{1}H-NMR spectra of the complexes revealed dramatic conformational changes throughout the host molecule (Table 2), which suggests a strong induced-fit binding mechanism. In the 2D-ROESY spectrum, nOe contacts between the protons of the guests and of the cavity proved their coordination inside the cavity. Despite the occurrence of large geometrical rearrangements, the measured association constants are high (K_a for **P4** = 3.1 × 10^4 M^{-1}, K_a for **P5** = 2.8 × 10^4 M^{-1}). The X-ray structures of both complexes could be determined, and these demonstrated the nearly perfect fit of the guests inside of the cavity of **Zn1** (Figure 5). In both complexes, **Zn1** has adopted a fully stretched conformation, and the lower aromatic rings of the guests are located in between the cavity side-walls, the average distances between these aromatic rings being 3.26 Å in the complex of **Zn1** with **P4** and 3.39 Å in the complex with **P5**, respectively. In accordance with literature examples of complexes between Zn(II) porphyrins and pyridine-based ligands,[41-43] the zinc ion is tilted out of the porphyrin surface in the direction of the pyridine ligand (typically 0.29 Å) and the bond distance between the zinc ion and the pyridine nitrogen atom is 2.1 Å. The stretched conformation of **Zn1** in the X-ray structures of the complexes is in agreement with the downfield-shifted resonances in the NMR spectra of protons H-3 and H-4, which are pushed away from the porphyrin upon binding of **P4** and **P5**. The resonances of H-8 and H-9 displayed upfield shifts, whereas the signals of H-6 and H-7 shifted downfield (Table 2). These shifts are clearly the result of **Zn1** adopting a stretched conformation upon the binding of **P4** and **P5**, which brings protons H-8 and H-9 closer to the shielding porphyrin plane than H-6 and H-7, whereas in unoccupied **Zn1**, H-6 and H-7 are located much closer to the porphyrin. The cavity of **Zn1** in the complex with **P5** is slightly more

stretched (0.25 Å) than in the complex with **P4**, which is the result of the difference in size between these guests. A careful look at Table 2 reveals that this more stretched conformation of the complex with **P5** compared to the complex with **P4** is also apparent from the different complexation induced shift values (the resonances of H-3, H-4 and H-5 are located more downfield in the complex with **P5** compared to the complex with **P4**), which indicates that the complexation geometry in solution is similar to that in the crystal.

Table 2 Selected ^{1}H NMR resonances for the protons of **$H_2$1**, **Zn1** and **Zn1** host-guest complexes between **Zn1** and **P1**, **P3**, **P4** and **P5**.[a,b]

Proton	**$H_2$1**	**Zn1**	**Zn1+P1**	**Zn1+P3**	**Zn1+P4**	**Zn1+P5**
H-3	6.95	6.52	6.95	6.98	7.02	7.07
H-4a	5.76	3.37	5.75	5.82	5.88	5.95
H-4b	6.48	3.44	6.46	6.51	6.66	6.72
H-5	6.39	5.84	6.38	6.44	6.15	6.28
H-6a	2.87	2.80	2.83	3.32	3.09	3.01
H-6b	3.26	3.22	3.25	3.42	3.27	3.17
H-7a	2.28	2.42	2.27	3.06	3.08	3.01
H-7b	2.49	2.58	2.46	3.06	3.17	3.13
H-8a	2.91	2.83	2.86	3.02	2.52	2.47
H-8b	3.01	2.92	2.97	3.02	2.70	2.65
H-9a	4.02	3.90	3.97	3.90	3.69	3.62
H-9b	4.14	4.03	4.09	4.01	3.75	3.68

[a]Determined by ^{1}H NMR experiments in $CDCl_3/CD_3CN$ 1:1 (v/v) solution. For proton numbering see Figure 1. [b]Chemical shifts of the complexes upon full binding of the ligand.

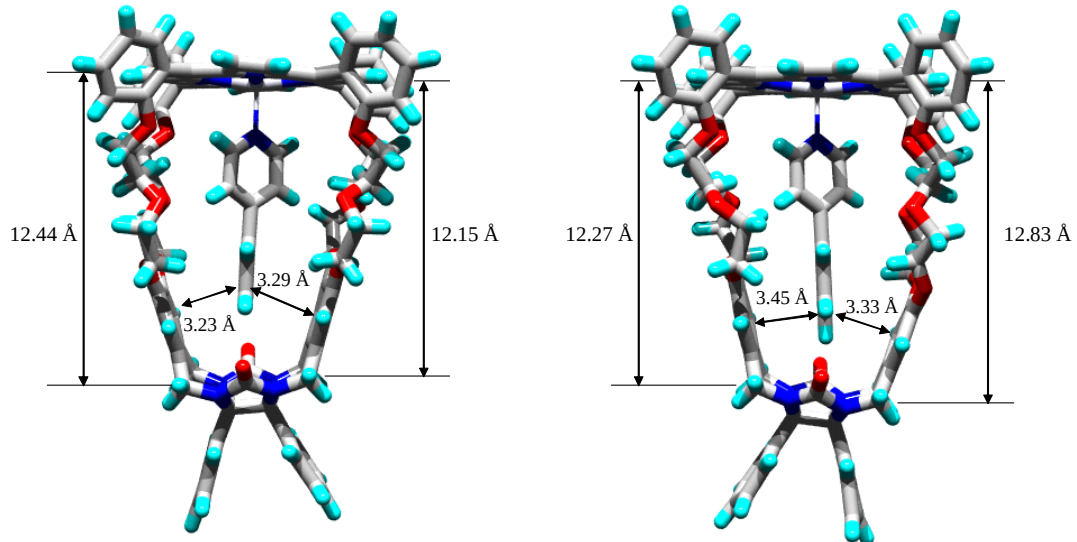

(*a*) (*b*)

Figure 5 X-ray structures of the complexes between (*a*) **Zn1** and **P4**, and (*b*) **Zn1** and **P5**. The dimensions of the cavity and distances between the side-walls and the guests are indicated in the images. See the Supporting Information for crystal data and procedures.

Binding of viologen derivatives. In addition to the binding of pyridine ligands to **Zn1**, also the binding of viologen molecules **V1**-**V5** in the cavity of **H$_2$1** was investigated. In all cases, NMR and UV-vis binding experiments revealed the formation of 1:1 complexes. Upon binding of the guests, large downfield shifts were observed for the crown ether-like spacer proton resonances (H-6, H-7, H-8 and H-9) in the ^{1}H NMR spectra, indicating that these protons move away from the porphyrin plane. Simultaneously, large upfield shifts ($\Delta\delta$ = –0.97 to –1.08 ppm) were observed for the pyrrole NH resonances as a result of shielding by the aromatic surfaces of the guests, which are therefore proposed to bind parallel and in close proximity to the porphyrin surface (Figure 6).[45] The large changes in the NMR spectra of **H$_2$1** upon the binding of the viologen guests indicate the occurrence of induced-fit binding mechanisms. The calculated association constants are high (Table 3) and in the same order of magnitude as the binding of **V1** to **H$_2$2** (K_a = 6.0 × 10^5 M^{-1}).[13] Clearly, the binding geometry of **V1** in **H$_2$1** is different than that of **V2**-**V4** in this host, which can be concluded from the completely different complexation induced shift (CIS) values that are observed for the complexes (Table 4), and from the significantly higher association constant for the complex between **H$_2$1** and **V1** (Table 3).

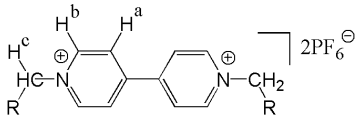

V1 R = H
V2 R = CH_3
V3 R = C_8H_{17}
V4 R = $C_{15}H_{31}$
V5 R = C_4H_8O

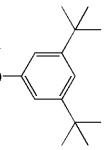

Table 3 Association constants K_a and binding free energies ΔG^o of complexes between **$H_2$1** and viologen derivatives **V1**-**V5**.

Guest	K_a (M^{-1})	ΔG^o (kJ $mole^{-1}$)
V1[a,b]	(6.4 ± 0.8) × 10^5	–33.1
V2[a]	(1.2 ± 0.2) × 10^5	–29.0
V3[a,b]	(1.0 ± 0.2) × 10^5	–28.5
V4[b,c]	(1.1 ± 0.2) × 10^5	–28.8
V5[b]	(1.0 ± 0.5) × 10^5	–28.5

[a]Determined by UV-vis titrations in $CHCl_3/CH_3CN$ 1:1 (v/v), [b]determined by fluorescence titrations in $CHCl_3/CH_3CN$ 1:1 (v/v), [3]determined by ^{1}H NMR experiments in $CDCl_3/CD_3CN$ 1:1 (v/v) and based on the integrated values of the free components and the complex, at T = 298 K.

Table 4 Selected calculated complexation induced shift (CIS) values Δδ (ppm) of host and guest proton signals upon the binding of viologens **V1**-**V5** in host **$H_2$1**.[a]

Proton	**V1**	**V2**	**V3**	**V4**	**V5**
H-6a	+0.89	+0.35	+0.34	+0.35	+0.35
H-6b	+0.24	+0.35	+0.35	+0.34	+0.35
H-7a	+1.26	+1.35	+1.35	+1.34	+1.36
H-7b	+1.30	+0.95	+0.94	+0.95	+0.95
H-8a	+0.89	+0.88	+0.88	+0.88	+0.88
H-8b	+0.95	+0.64	+0.64	+0.63	+0.63
H-9a	+0.49	+0.77	+0.78	+0.77	+0.79
H-9b	+0.63	+0.21	+0.18	+0.19	+0.18
H-13	–0.45	–0.18	–0.16	–0.17	–0.18
H-16	–1.08	–1.00	–0.98	–0.98	–0.97
H^a	–3.80	–2.98	–2.85	–2.86	–2.89
H^b	–1.16	–1.74	–1.88	–1.89	–1.86
H^c	–0.56	[b]	–1.33	–1.32	–1.28

[a]Determined by ^{1}H NMR experiments in $CDCl_3/CD_3CN$ 1:1 (v/v). For proton numbering see Figure 1 and Chart 3. [b]CIS value could not be determined because the signal was obscured by other proton resonances.

The flexible, electron-rich crown ether-like spacers play a crucial role in the accommodation of the electron-deficient viologen guests. Molecular modeling indicates that two binding geometries of a viologen guest in **H$_2$1**, in which it is oriented parallel to the porphyrin plane, are possible (Figure 6). In the "pseudo-rotaxane geometry" the crown ether-like oxygen atoms are facing the inside of the cavity, thereby stabilizing the positive charges of the viologen. In the so-called "suit(2)ane geometry",[46] the positive charges of the viologen guest are located in between the two crown ether-like rings between the cavity side-walls and the porphyrin. In order to force viologen complexation in the rotaxane geometry, **V5** was added to **H$_2$1**. The bulky blocking groups of this guest can only be traversed by the full dimension of the cavity and the geometry of the resulting host-guest complex can therefore only be rotaxane-like, as in Figure 6a. The formation of the complex of **H$_2$1** with **V5** was found to occur via a so called 'slippage' mechanism: in order to bind the guest, **H$_2$1** first needs to slip over one of the two blocking groups thereby mounting a high activation barrier.[47-51] At NMR concentrations ($\approx 10^{-3}$ M), it takes several days before the components reach complexation equilibrium.[52] The ^{1}H NMR and 2D-ROESY spectra of the complex are strikingly similar to the spectra of the complexes between **H$_2$1** and **V2**-**V4** (Table 4), which therefore indicates that all these derivatives have pseudo-rotaxane complexation geometries.

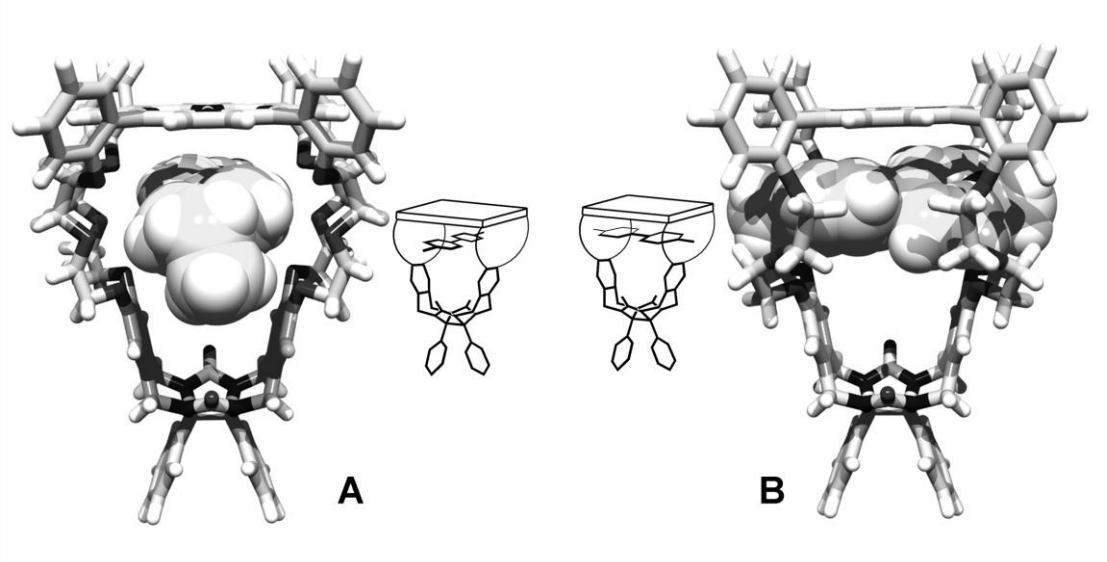

Figure 6 Computer-modeled structures and cartoons of (A) the "pseudo-rotaxane geometry" of the complex between **H$_2$1** and **V2** and (B) the "suit(2)ane geometry" of the complex between **H$_2$1** and **V1**, based on the ^{1}H, COSY and 2D-ROESY NMR spectra.

The complex between **H$_2$1** and **V1**, on the other hand, was found to have a suitane geometry (Figure 6b). nOe contacts are observed between the host protons H-14 and H-9a/H-9b (see Figure 1), and between H-15 of the host and Hc of **V1**, whereas in the complexes of **H$_2$1** with **V2**-**V5**, H-15 has nOe contacts with H-9b and H-14 with Hc of **V3**-**V5**. The crown ether-like proton signals furthermore appeared to be very diagnostic for identifying either a rotaxane or a suitane geometry (Figure 7). For instance, in the

suitane geometry H-9a experiences more shielding from the porphyrin plane than H-9b, whereas in the rotaxane complexes H-9b is more shielded than H-9a. An attempt was undertaken to convert a complex with rotaxane geometry into a complex with suitane geometry. To this end, **V1** was titrated into a solution containing a 1:1 complex between **H$_2$1** and **V2** (Figure 7c). The observed changes in the NMR spectra indeed indicated the formation of the suitane complex between **H$_2$1** and **V1** at the expense of the rotaxane complex between **H$_2$1** and **V2**, confirming the above described interpretations of the NMR data. In addition, the competition experiment revealed that **V1** binds five times stronger to **H$_2$1** than **V2**, in line with the obtained values for the association constants (Table 3).

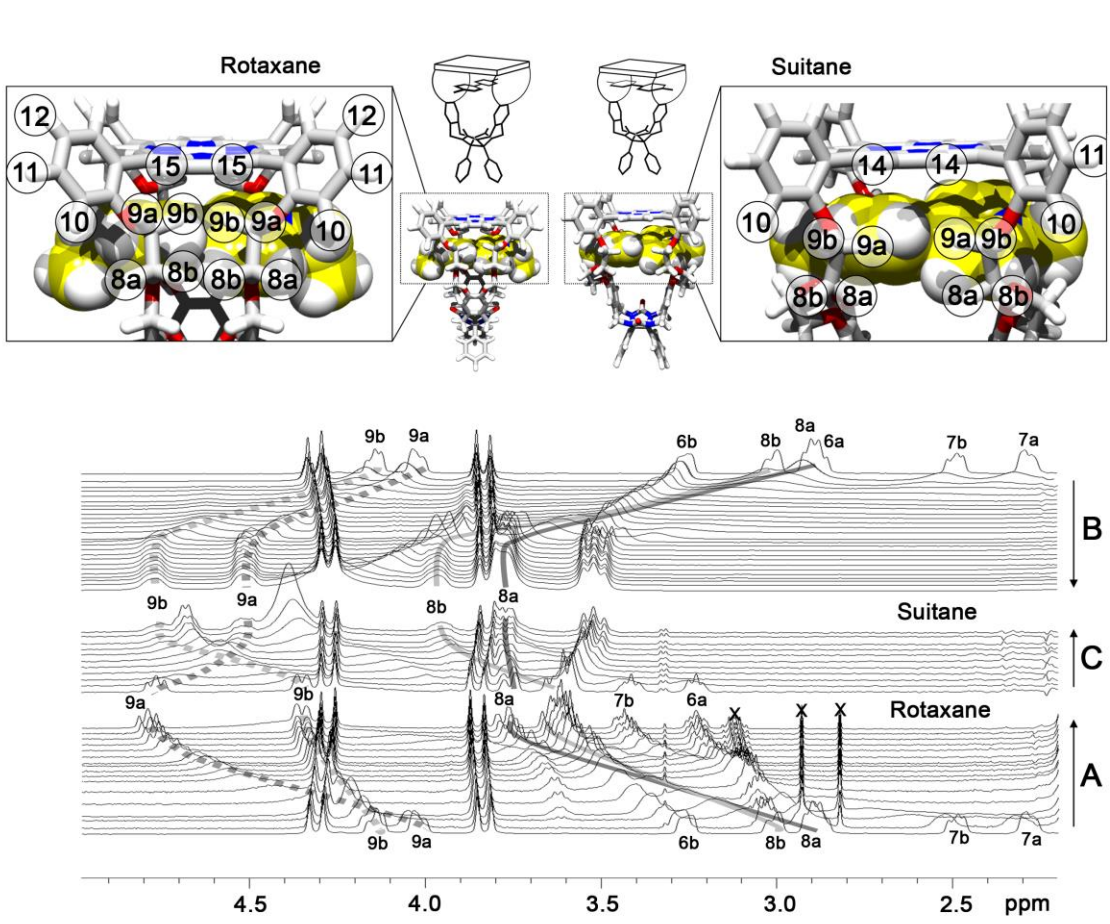

Figure 7 ^{1}H-NMR spectra of **H$_2$1** with various amounts of guests **V1** and **V2** in $CDCl_3/CD_3CN$ 1:1 (v/v). (A) From bottom to top increasing amounts of **V2**, (B) from top to bottom increasing amounts of **V1**, (C) from bottom to top increasing amounts of **V1** to a mixture of **H$_2$1** and **V2**. The exchanging signals of most of the proton resonances can be followed (lines are added as a guide to the eye).

Comparison of the complexes. Binding of pyridine and viologen guests in host **1** occurs via induced-fit mechanisms similar to those observed for the binding of these guests in flexible host **3**. Although the flexible host **1** lacks the preorganisation of rigid host **2**, the association constants obtained for different guests are similar for both hosts, which is somewhat surprising because binding inside the cavity of **1** is accompanied by severe conformational changes. It can therefore be concluded that the binding strength

mainly depends on the possibility of **1** to provide the guests with extra stabilizing interactions. Pyridine (**P3**) coordinates strongly on the inside of hosts **Zn2** (K_a = 1.1 × 10^5 M^{-1}) and **Zn3** (K_a = 1.4 × 10^4 M^{-1}) as a result of highly favourable π–π interactions between the cavity side-walls and the aromatic surface of the guest, in addition to the zinc-nitrogen coordination. Although **P3** also coordinates on the inside of the cavity of **Zn1**, this host cannot provide the guest with such stabilizing π–π interactions, which results in a significantly lower association constant. In contrast, guests **P4** and **P5** completely fill the cavity of **Zn1** and experience, in addition to ideal van der Waals interactions, strong π–π interactions with the cavity side-walls, which results in stronger binding. The association constants between **V1** and **H₂1** (K_a = 6.4 × 10^5 M^{-1}) and **V1** and **H₂2** (K_a = 6.0 × 10^5 M^{-1} are several orders of magnitude larger than that observed for the binding of this guest to **H₂3** (K_a = 1100 M^{-1}). In the complexes with the former two hosts, **V1** is bound in a very tight geometry. **H₂1** accommodates the positive charges of **V1** between the two crown ether-like rings and the complex is further stabilized by additional π–π interactions between the porphyrin and the guest. In **H₂2**, **V1** is clamped between the cavity side-walls, which provide stabilizing π–π interactions in addition to electrostatic interactions between the crown ether-like oxygen atoms and the positive charges of the guest. The crown ether-like rings of host **H₂3** are oriented too wide to favourable wrap themselves around **V1**, which results in weaker binding. The differences in binding strength between the complexes of the different viologen guests with host **H₂1** (Table 2) can also be explained in this way. In the suitane geometry of the complex between **V1** and **H₂1**, the guest is bound more tightly when compared to the more loosely bound guests **V2-V5** in the rotaxane geometry, resulting in a higher association constant observed for **V1**.

Conclusion

The flexibility of the new porphyrin hosts **H₂1** and **Zn1** is expressed in their complex conformational behaviour upon the binding of guests. Insertion of a zinc ion in the porphyrin causes a structural change in the host cavity which is attributed to an intramolecular coordination between the zinc ion and the oxygen atoms in the crown ether-like spacers. The binding of guests on the inside of the cavities induces large conformational changes throughout the hosts. Despite the binding of guests via induced-fit mechanisms, in many cases still high association constants are obtained, which shows that not only ‘lock and key’, but also ‘induced-fit’ binding can lead to the formation of strong complexes.

Experimental Section

General. All syntheses were carried out under an inert nitrogen or argon atmosphere. Chloroform and acetonitrile used in titration experiments were distilled from $CaCl_2$. Dichloromethane, 1,2-dichloroethane,

and methanol were distilled from CaH_2. Pyrrole was purified over a plug of alumina prior to use. Salicylic aldehyde was vacuum distilled. Catechol was recrystallized from dichloromethane prior to use. $MgSO_4$ and K_2CO_3 were dried in an oven (150ºC). All other solvents and chemicals were commercial materials and used as received. Merck silica gel (60H) was used for column chromatography, and Merck silica gel F254 plates were used for thin layer chromatography and preparative TLC. Molecular modeling calculations were performed with the use of Spartan. Fluorescence experiments were performed on a Perkin-Elmer LS50B luminescent spectrometer equipped with a thermostatted cuvette holder. UV-vis spectra were recorded on a Cary 100 Conc (Varian, Middelburg) UV-Vis spectrometer. Maldi-TOF ms was performed on a Bruker Biflex III spectrometer. NMR spectra were taken on a Varian Inova 400 (400 MHz, ^{1}H and 2D spectra) or on a Bruker DMX300 (75 MHz, ^{13}C spectra) and calibrated to an internal standard of tetramethylsilane. Abbreviations used are s, singlet; d, doublet; t, triplet; dd, double doublet; m, multiplet. Ditosylate **7**.[34,35] tetrakis(chloromethyl) diphenylglycoluril **8**[36] methyl viologen **V1** and double blocked viologen **V5**[18] were synthesized according to literature procedures.

Syntheses.

Tetra tosyl host molecule (9): Compounds **7** (4.5 g, 7.6 mmol) and **8** (1.8 g, (3.8 mmol) were dissolved in freshly distilled 1,2-dichloroethane (300 mL). $SnCl_4$ (4 mL, 32 mmol) was added and the mixture was refluxed under argon for 16 hours. After cooling, aqueous 6N HCl (10 mL) was added and the mixture was refluxed for another 30 min. After cooling CH_2Cl_2 (100 mL) was added and the organic layer was washed with aqueous 1N HCl (3 × 100 mL) and water and evaporated to dryness. After purification by column chromatography (50% to 70% EtOAc in toluene (v/v)) and crystallization from nitromethane, **9** was obtained as a white solid (1.37 g, 23%). ^{1}H NMR ($CDCl_3$, 400 MHz): δ 7.76 (d, 8H, ^3J(H,H) = 8.3 Hz), 7.24 (d, 8H, ^3J(H,H) = 8.2 Hz), 7.17-7.10 (m, 10H, Ar*H* glycoluril), 6.76 (s, 4H, side-wall), 4.69 (d, 4H, ^2J(H,H) = 15.9 Hz), 4.20-4.10 (m, 12H), 3.88-3.83 (m, 8H), 3.69-3.66 (m, 8H), 3.65-3.61 (m 8H), 2.24 (s, 12H). ^{13}C NMR ($CDCl_3$, 75 MHz): δ 157.27, 146.88, 144.38, 133.17, 132.42, 130.03, 129.65, 129.31, 128.36, 128.22, 127.78, 127.47, 115.77, 84.94, 69.21, 68.98, 68.28, 44.44, 20.93. Maldi-TOF MS (m/z): 1532 $(M)^+$.

Free base porphyrin host ($H_2$1): A suspension of **9** (120 mg, 0.078 mmol), 5,10,15,20-tetrakis(*meso-p*-hydroxyphenyl)porphyrin **10** (53 mg, 0.078 mmol) and K_2CO_3 (100 mg, 0.72 mmol) in DMF (250 mL) was reacted for 16 h under argon atmosphere at 110ºC. After cooling, filtration of the salts and evaporation of the solvent the product was purified by column chromatography (3% MeOH in $CHCl_3$ (v/v)) followed by preparative TLC (7/7/1 toluene/EtOAc/MeOH (v/v/v). The product was dissolved in a minimal amount of $CHCl_3$ and to this solution *n*-hexane was added. A precipitate was formed which was collected by centrifugation and dried under vacuum yielding 16 mg (13%) of **$H_2$1** as a purple solid.

M.p.>300ºC (dec). ^{1}H NMR ($CDCl_3$ 400 MHz): δ 8.79 (s, 4H), 8.77 (s, 4H), 8.05 (d, 4H, ^3J(H,H) = 7.1 Hz), 7.75 (t, 4H, Ar*H*, ^3J(H,H) = 7.7 Hz), 7.4-7.35 (m, 8H, Ar*H*), 7.03-6.96 (m, 6H), 6.93-6.90 (m, 4H), 6.37 (s, 4H), 4.30 (d, 4H, ^2J(H,H) = 15.6 Hz), 4.17-4.11 (m, 4H), 4.00-3.94 (m, 4H), 3.79 (d, 4H, J = 15.5 Hz), 3.12-3.06 (m, 4H), 3.01-2.95 (m, 4H), 2.87-2.81 (m, 4H), 2.69-2.64 (m, 4H), 2.14-2.08 (m, 4H), 1.92-1.86 (m, 4H), -2.62 (s, 2H, N*H*); see Figure 1 for proton assignments. ^{13}C NMR ($CDCl_3$, 75 MHz): δ 159.23, 157.36, 146.50, 135.42, 133.99, 131.71, 130.25, 129.80, 128.69, 128.50, 127.96, 119.93, 118.75, 115.61, 113.20, 85.30, 70.05, 69.32, 68.43, 68.33, 44.30. Maldi-TOF MS (m/z): 1522 $(M)^+$. HR-ESI-MS calcd for $[C_{92}H_{80}N_8O_{14} + H]^+$: 1521.58722. Found: 1521.58410. calcd for $[C_{92}H_{80}N_8O_{14} + Na]^+$: 1543.56917. Found: 1543.57147.

Zinc porphyrin host (Zn1): Compound **$H_2$1** (10 mg, 6.6 μmol) and zinc acetate dihydrate (50 mg 0.23 mmol) were dissolved in a mixture of MeOH and CH_2Cl_2 (1:1 (v/v), 10 mL). The mixture was stirred at room temperature for one hour. The solvents were evaporated and the salts were removed by chromatography over a plug of silica (eluent MeOH/$CHCl_3$ 1:10 (v/v)). After precipitation in *n*-hexane, 10 mg (96%) of **Zn1** was obtained as a purple solid. M.p.>300ºC. ^{1}H NMR ($CDCl_3$ 400 MHz): δ 8.83 (s, 4H), 8.79 (s, 4H), 7.93 (br s, 4H), 7.69 (t, 4H, ^3J(H,H) = 7.2 Hz), 7.36 (d, 4H, ^3J(H,H) = 8.1 Hz), 7.24 (br s, 4H) 7.05-6.99 (m, 6H), 6.61 (br , 4H), 6.98 (br s, 4H), 4.02 (br s, 4H), 3.89 (br s, 4H), 3.67 (br s, 4H), 3.47 (br s, 4H), 3.11 (br s, 4H), 2.82 (br s, 4H), 2.78 (br s, 4H), 2.59 (br s, 4H), 2.20 (br s, 4H), 1.95 (br s, 4H); see Figure 3 for proton assignments. ^{13}C NMR ([D_6]DMSO, 75 MHz): δ 158.78, 156.55, 149.25, 149.14, 146.58, 135.72, 133.29, 132.28, 130.99, 130.43, 129.50, 128.56, 128.48, 127.74, 119.69, 116.99, 115.81, 113.81, 84.49, 69.04, 68.89, 68.57, 68.45, 43.83. Maldi-TOF MS (m/z): 1585 $(M)^+$.

4-(tert-Butyl-diphenyl-silanyloxymethyl)-pyridine (P1): 4-Pyridylcarbinol (1.0 g, 9.2 mmol) and imidazole (1.0 g, 14.7 mmol), were dissolved in CH_2Cl_2 (50 mL) and to this solution was slowly added *tert*-butyl-chlorodiphenyl-silane (3.0 g, 11 mmol). The mixture was stirred at room temperature for 4 h, washed with water, the organic layer was concentrated and the product was purified by column chromatography (50% EtOAc/CH_2Cl_2 (v/v)). Crystallization from nitromethane yielded 2.1 g (6.04 mmol, 66%) of **P1** as a colourless solid. ^{1}H NMR ($CDCl_3$ 400 MHz): δ 8.56 (d, 2H, Ar*H*, ^3J(H,H) = 5.2 z), 7.67 (d, 4H, ^3J(H,H) = 7.2 Hz), 7.35-7.47 (m, 6H), 7.28 (d, 2H, ^3J(H,H) = 5.2 Hz), 4.76 (s, 2H), 1.12 (s, 9H). ^{13}C NMR ($CDCl_3$ 75 MHz): δ 150.0, 149.7, 135.5, 132.9, 129.9, 127.8, 120.6, 64.1, 26.8, 19.3. HR-ESI-MS calcd for $C_{22}H_{36}NOSi^+$: 348.17837. Found: 348.17888.

(*N*,*N*')-Diethyl-4,4'-bipyridinium dihexafluorophosphate (V2): 4,4'-Bipyridine (0.5 g, 6.4 mmol) and iodo-ethane (1 mL, excess) were stirred for 24 h in DMF (20 mL). Diethyl ether (50 mL) was added, the resulting precipitate was filtered off, washed with diethyl ether, and dried under vacuum. The product was dissolved in a minimal amount of water, and this solution was then added to a saturated aqueous NH_4PF_6

solution to yield, after filtration, washing with water, and drying under vacuum, 1.1 g (68%) of **V2** as a white solid. ^{1}H NMR ($CDCl_3$/CD_3CN 1:1 (v/v) 400 MHz): δ 8.94 (d, 4H, ^{3}J(H,H) = 6.9 Hz), 8.41 (d, 4H, ^{3}J(H,H) = 6.3 Hz), 4.70 (q, 4H, ^{3}J(H,H) = 7.4 Hz), 1.69 (t, 6H, ^{3}J(H,H) = 7.3 Hz).

(*N*,*N*')-Dinonyl-4,4'-bipyridinium dihexafluorophosphate (V3): 4,4'-Bipyridine (300 mg, 1.92 mmol) and 2-bromononane (2.0 g, 9.7 mmol) were refluxed in CH_3CN (20 ml) for 24 h. After cooling, the formed precipitate was filtered off, washed with diethyl ether, and dried under vacuum. The product was dissolved in a minimal amount of water, and this solution was then added to a saturated aqueous NH_4PF_6 solution to yield, after filtration and drying under vacuum, 310 mg (23 %) of **G2** as a white solid. ^{1}H NMR ($CDCl_3$/CD_3CN 1:1 (v/v) 400 MHz): δ 8.93 (d, 4H, Ar*H*, ^{3}J(H,H) = 6.8), 8.42 (d, 4H, Ar*H*, ^{3}J(H,H) = 6.5 Hz), 4.62 (t, 4H, NCH_2, ^{3}J(H,H) = 7.6 Hz), 2.00-2.06 (m, 4H, NCH_2CH_2), 1.35-1.42 (m, 8H, CH_2), 1.25-1.35 (m, 16H, CH_2), 0.89 (t, 6H, CH_3, ^{3}J(H,H) = 6.8 Hz). Maldi-TOF MS (m/z) 410.79 (M-2PF_6^-).

(*N*,*N*')-Dipentadecyl-4,4'-bipyridinium dihexafluorophosphate (V4): 4,4'-Bipyridine (300 mg, 1.92 mmol) and 2-bromopentadecane (3.0 g, 10.3 mmol) were refluxed in CH_3CN (15 ml) for 24 h. After cooling, the formed precipitate was filtered off, washed with diethyl ether, and dried under vacuum. The product was dissolved in a minimal amount of water, and this solution was then added to a saturated aqueous NH_4PF_6 solution to yield, after filtration and drying under vacuum, 467 mg (28%) of **G2** as a white solid. ^{1}H NMR ($CDCl_3$/CD_3CN 1:1 (v/v) 400 MHz): δ 8.91 (d, 4H, ^{3}J(H,H) = 7.0 Hz), 8.41 (d, 4H, ^{3}J(H,H) = 6.7 Hz), 4.62 (t, 4H^{3}J(H,H) = 7.6 Hz), 2.00-2.05 (m, 4H), 1.36-1.42 (m, 8H), 1.22-1.33 (m, 44H), 0.88 (t, 6H, ^{3}J(H,H) = 6.9 Hz).

Acknowledgements

This research was supported by a National Research School Combination Catalysis Controlled by Chemical Design grant, Nederlandse Organisatie voor Wetenschappelijk Onderzoek Vidi (J.A.A.W.E., A.E.R.) and Vici (A.E.R.) grants, an ERC Starting Grant (J.A.A.W.E.), a Koninklijke Nederlandse Akademie van Wetenschappen grant (R.J.M.N.),an ERC Advanced grant (R.J.M.N.), a NanoNed grant (A.E.R. and R.J.M.N.), and a grant from the Ministry of Education, Culture and Science (Gravity program 024.001.035).

References and Notes

[1] Supramolecular Catalysis. Edited by P. W. N. M. van Leeuwen **2008** WILEY-VCH Verlag GmbH & Co. KGaA, Weinheim ISBN: 978-3-527-32191-9.

[2] Kuroda, Y.; Hiroshige, T.; Sera, T.; Shiroiwa, Y.; Tanaka, H.; Ogoshi, H. *J. Am. Chem. Soc.* **1989**, *111*, 1912-1913.

[3] Kuroda, Y.; Ito, M.; Sera, T.; Ogoshi, H. *J. Am. Chem. Soc.* **1993**, *115*, 7003-7004.

[4] Bonar-Law, R. P.; Sanders, J. K. M. *J. Am. Chem. Soc.* **1995**, *117*, 259-271.

[5] Bonar-Law, R. P.; Sanders, J. K. M. *J. Chem. Soc., Perkin Trans. 1* **1995**, 3085-3096.

[6] Rudkevich, D. M.; Verboom, W.; Reinhoudt, D. N. *Tetrahedron Lett.* **1994**, *35*, 7131-7134.

[7] Rudkevich, D. M.; Verboom, W.; Reinhoudt, D. N. *J. Org. Chem.* **1995**, *60*, 6585-6587.

[8] Nagasaki, T.; Fujishima, H.; Takeuchi, M.; Shinkai, S. *J. Chem. Soc., Perkin Trans. 1* **1995**, 1883-1888.

[9] Reek, J. N. H.; Rowan, A. E.; Crossley, M. J.; Nolte, R. J. M. *J. Org. Chem.* **1999**, *64*, 6653-6663.

[10] Benson, D. R.; Valentekovich, R.; Knobler, C. B.; Diederich, F. *Tetrahedron* **1991**, *47*, 2401-2422.

[11] Anderson, S.; Anderson, H. L.; Bashall, A.; McPartlin, M.; Sanders, J. K. M. *Angew. Chem., Int. Ed. Engl.* **1995**, *34*, 1096-1099.

[12] Collman, J. P.; Zhang, X.; Hembre, R. T.; Brauman, J. I. *J. Am. Chem. Soc.* **1990,** *112*, 5357-5359.

[13] Elemans, J. A. A. W.; Claase, M. B.; Aarts, P. P. M.; Rowan, A. E.; Schenning, A. P. H. J.; Nolte, R. J. M. *J. Org. Chem.* **1999**, *64*, 7009-7016.

[14] Elemans, J. A. A. W.; Bijsterveld, E. J. A.; Rowan, A. E.; Nolte. R. J. M. *Eur. J. Org. Chem.* **2007**, 751–757.

[15] Elemans, J. A. A. W.; Bijsterveld, E. J. A.; Rowan, A. E.; Nolte, R. J. M. *Chem. Commun.* **2000**, 2443-2444.

[16] Trakselis, M. A.; Alley, S. C.; Abel-Santos, E.; Benkovic, S. J. *Proc. Natl Acad. Sci. USA* **2001**, *98*, 8368–8375, Kovall, R.; Matthews, B. W. *Science* **1997**, *277*, 1824–1827.

[17] Thordarson, P.; Bijsterveld, E. J. A.; Rowan, A. E.; Nolte, R. J. M. *Nature* **2003**, *424*, 915-918.

[18] Coumans, R. G. E.; Elemans, J. A. A. W.; Nolte, R J. M.; Rowan, A E. *Proc. Natl. Acad. Sci.* **2006**, *103*, 19647-19651.

[19] Dalla Cort, A.; Mandolini, L.; Schiaffino, L. *Chem. Commun* **2005**, 3867–3869.

[20] Zhang, B. L.; Breslow, R. *J. Am. Chem. Soc.* **1997**, *119*, 1676-1681.

[21] Mattei, P.; Diederich, F. *Helv. Chim. Acta* **1997**, *80*, 1555-1588.

[22] Diederich, F.; Lutter, H. D. *J. Am. Chem. Soc.* **1989**, *111* , 8438-8446.

[23] Ortega-Caballero, F.; Rousseau, C.; Christensen, B.; Ellebæk Petersen, T.; Bols, M. *J. Am. Chem. Soc.* **2005**, *127*, 3238-3239.

[24] Yoshizawa, M.; Tamura, M.; Fujita, M. *Science,* **2006**, *312*, 251-254.

[25] Hooley, R. J.; Biros, S. M.; Rebek, J. Jr. *Angew. Chem., Int. Ed.* **2006**, *45*, 3517-3519.

[26] Fiedler, D.; Bergman, R. G.; Raymond, K. N. *Angew. Chem. Int. Ed.* **2004**, *43*, 6748 –6751.

[27] Fiedler, D.; van Halbeek, H.; Bergman, R. G.; Raymond, K. N. *J. Am. Chem. Soc.* **2006**, *128*, 10240-10252.

[28] Fischer, E.; *Ber. Dtsch. Chem. Ges.* **1894**, *27*, 2984-2993.

[29] Pauling, L. *Chem. Eng. News* **1946**, *24***,** 1375–1377.

[30] Koshland, D. E.; *Proc. Natl. Acad. Sci. USA* **1958**, *44*, 98-104.

[31] Berger, C.; Weber-Bornhauser, S.; Eggenberger, J.; Hanes, J.; Plückthun, A.; Bosshard, H. R. *FEBS Lett.* **1999**, *450*, 149–153.

[32] Bosshard, H. R.; *News Physiol. Sci.* **2001**, *16*, 171-173.

[33] Sanders, J. K. M. *Chem. Eur. J.* **1998**, *4*, 1378-1383.

[34] Wright, K.; Melandri, F.; Cannizzo, C.; Wakselman, M.; Mazaleyrat, J. P. *Tetrahedron* **2002**, *58*, 5811-5820.

[35] Weber, E. *Liebigs Ann. Chem.* **1983**, *5*, 770-801.

[36] Sijbesma, R. P.; Nolte, R. J. M. *Recl. Trav. Chim. Pays-Bas* **1993**, *112*, 643-647.

[37] Absorbance maxima and association constants of dioxane, THF, Et_2O, Acetone and diethylether to reference zinc porphyrins 5,10,15,20-tetrakis-(2-methoxy-phenyl)-Zn-porphyrin (**Zn4**) and 5,10,15,20-tetrakis-(3-methoxy-phenyl)-Zn-porphyrin (**Zn5**) in chloroform.

Zn4 chloroform (Soret: 420 nm, Q-bands: 548, 585 nm),
Zn4 + THF K_a = 12 M^{-1} (Soret: 425 nm, Q-bands: 556, 594 nm),
Zn4 + [1,4]dioxane K_a = 63 M^{-1} (Soret: 424 nm, Q-bands: 553, 591 nm),
Zn4 + acetone (Soret: 422 nm, Q-bands: 552, 592 nm),
Zn4 + diethylether K_a = 9.0 M^{-1} (Soret: 426 nm, Q-bands: 554, 596 nm),
Zn5 + chloroform (Soret: 420 nm, Q-bands: 546, 585 nm),
Zn5 + THF K_a = 20 M^{-1} (Soret: 425 nm, Q-bands: 556, 596 nm),
Zn5 + dioxane K_a = 32 M^{-1} (Soret: 424 nm, Q-bands: 552, 593 nm),
Zn5 + diethylether K_a = 0.7 M^{-1} (Soret: 423 nm, Q-bands: 553, 593 nm),
Zn5 + acetone K_a = 0.4 M^{-1} (Soret: 423 nm, Q-bands: 553, 592 nm).

]38] Michaudet, L.; Philippe Richard, P.; Boitrel, B. *Tetrahedron. Lett.* **2000**, *41*, 8289–8292.

[39] Hunter, C. A.; Sanders, J. K. M. *J. Am. Chem. Soc.* **1990**, *112*, 5525-5534.

[40] Calculated association constants of pyridine with 5,10,15,20-tetrakis-(2-methoxy-phenyl)-Zn-porphyrin and 5,10,15,20-tetrakis-(3-methoxy-phenyl)-Zn-porphyrin in acetonitrile/chloroform 1:1 (v/v) are $K_a = 1.4 \times 10^3$ M^{-1} and $K_a = 1.0 \times 10^3$ M^{-1} respectively.

[41] Muniappan, S.; Liptsman, S.; Goldberg. I. *Acta Cryst.* **2006**, *C62*, m140-m143.

[42] Shukla, A. D.; Dave, P. C.; Suresh, E.; Das, A. Dastidar, P. *J. Chem. Soc*., *Dalton Trans*., **2000**, 4459–4463.

[43] Litvinov, A. L.; Konarev, D. V.; Kovalevsky, A. Y.; Neretin, I. S.; Coppens, P.; Lyubovskaya, R. N. *Crystal Growth & Design* **2005**, *5*, 1807-1819.

[44] For a good comparison of viologen binding to porphyrin hosts: Gunter, M. J.; Jeynes, T. P.; Johnston, M. R.; Turner, P.; Chen, Z. *J. Chem. Soc., Perkin Trans. 1*, **1998**, 1945-1957.

[45] Williams, A.R.; Northrop, B. H.; Chang, T.; Stoddart, J. F.; White, A. J. P.; Williams, D. J. *Angew. Chem. Int. Ed.* **2006**, *40*, 6665-6669.

[46] Ashton, P. R.; Bělohradsky, M.; Philp, D.; Stoddart, J. F. *J. Chem. Soc., Chem. Commun.* **1993**, *16*, 1269-1274.

[47] Ashton, P. R.; Bělohradsky, M.; Philp, D.; Spencer, N.; Stoddart, J. F. *J. Chem. Soc., Chem. Commun.* **1993**, *16*, 1274-1277.

[48] Amabilino, D. B.; Ashton, P. R.; Bělohradsky, M.; Raymo, F. M.; Stoddart, J. F. *J. Chem. Soc., Chem. Commun.* **1995**, *7*, 751-753.

[49] Bělohradsky, M.; Philp, D.; Raymo, F. M.; Stoddart, J. F. In *Organic Reactivity: Physical and Biological Aspects*; Golding, B. T.; Griffin, R. J.; Maskill, H.; Eds.; RSC Special Publication No. 148: Cambridge, **1995**; pp 387-398.

[50 Ashton, P. R.; Ballardini, R.; Balzani, V.; Bělohradsky, M.; Gandolfi, M. T.; Philp, D.; Prodi, L.; Raymo, F. M.; Reddington, M. V.; Spencer, N.; Stoddart, J. F.; Venturi, M.; Williams, D. J. *J. Am. Chem. Soc.* **1996**, *118*, 4931-4951.

[51] Slippage of this host over blocking groups will be described thoroughly in a separate paper.